

Observation of $B^+ \rightarrow p\bar{\Lambda}\gamma$

Y.-J. Lee,²³ M.-Z. Wang,²³ K. Abe,⁷ K. Abe,³⁸ H. Aihara,⁴⁰ Y. Asano,⁴⁴ V. Aulchenko,¹ T. Aushev,¹¹ S. Bahinipati,⁴ A. M. Bakich,³⁵ I. Bedny,¹ U. Bitenc,¹² I. Bizjak,¹² A. Bondar,¹ A. Bozek,²⁴ M. Bračko,^{7,17,12} J. Brodzicka,²⁴ T. E. Browder,⁶ M.-C. Chang,²³ P. Chang,²³ Y. Chao,²³ A. Chen,²¹ K.-F. Chen,²³ W. T. Chen,²¹ B. G. Cheon,³ R. Chistov,¹¹ S.-K. Choi,⁵ A. Chuvikov,³¹ S. Cole,³⁵ J. Dalseno,¹⁸ M. Danilov,¹¹ M. Dash,⁴⁵ A. Drutskoy,⁴ S. Eidelman,¹ Y. Enari,¹⁹ F. Fang,⁶ S. Fratina,¹² N. Gabyshev,¹ A. Garmash,³¹ T. Gershon,⁷ G. Gokhroo,³⁶ B. Golob,^{16,12} A. Gorišek,¹² J. Haba,⁷ K. Hayasaka,¹⁹ M. Hazumi,⁷ L. Hinz,¹⁵ T. Hokuue,¹⁹ Y. Hoshi,³⁸ S. Hou,²¹ W.-S. Hou,²³ Y. B. Hsiung,²³ T. Iijima,¹⁹ A. Imoto,²⁰ K. Inami,¹⁹ A. Ishikawa,⁷ R. Itoh,⁷ M. Iwasaki,⁴⁰ Y. Iwasaki,⁷ J. H. Kang,⁴⁶ J. S. Kang,¹³ P. Kapusta,²⁴ N. Katayama,⁷ H. Kawai,² T. Kawasaki,²⁶ H. R. Khan,⁴¹ H. Kichimi,⁷ H. J. Kim,¹⁴ S. K. Kim,³³ S. M. Kim,³⁴ K. Kinoshita,⁴ S. Korpar,^{17,12} P. Križan,^{16,12} P. Krokovny,¹ S. Kumar,²⁹ C. C. Kuo,²¹ A. Kuzmin,¹ Y.-J. Kwon,⁴⁶ G. Leder,¹⁰ S. E. Lee,³³ T. Lesiak,²⁴ J. Li,³² S.-W. Lin,²³ D. Liventsev,¹¹ F. Mandl,¹⁰ T. Matsumoto,⁴² A. Matyjka,²⁴ W. Mitaroff,¹⁰ H. Miyake,²⁸ H. Miyata,²⁶ R. Mizuk,¹¹ G. R. Moloney,¹⁸ T. Nagamine,³⁹ Y. Nagasaka,⁸ E. Nakano,²⁷ M. Nakao,⁷ H. Nakazawa,⁷ Z. Natkaniec,²⁴ S. Nishida,⁷ O. Nitoh,⁴³ S. Ogawa,³⁷ T. Ohshima,¹⁹ T. Okabe,¹⁹ S. L. Olsen,⁶ W. Ostrowicz,²⁴ H. Ozaki,⁷ H. Palka,²⁴ C. W. Park,³⁴ N. Parslow,³⁵ L. S. Peak,³⁵ R. Pestotnik,¹² L. E. Piilonen,⁴⁵ N. Root,¹ M. Rozanska,²⁴ H. Sagawa,⁷ Y. Sakai,⁷ N. Sato,¹⁹ T. Schietinger,¹⁵ O. Schneider,¹⁵ J. Schümann,²³ K. Senyo,¹⁹ M. E. Sevier,¹⁸ T. Shibata,²⁶ H. Shibuya,³⁷ B. Shwartz,¹ V. Sidorov,¹ J. B. Singh,²⁹ A. Somov,⁴ R. Stamen,⁷ S. Stanič,^{44,*} M. Starič,¹² K. Sumisawa,²⁸ T. Sumiyoshi,⁴² O. Tajima,⁷ F. Takasaki,⁷ K. Tamai,⁷ N. Tamura,²⁶ M. Tanaka,⁷ Y. Teramoto,²⁷ X. C. Tian,³⁰ T. Tsukamoto,⁷ S. Uehara,⁷ T. Uglov,¹¹ K. Ueno,²³ S. Uno,⁷ P. Urquijo,¹⁸ G. Varner,⁶ K. E. Varvell,³⁵ S. Villa,¹⁵ C. C. Wang,²³ C. H. Wang,²² M. Watanabe,²⁶ Q. L. Xie,⁹ A. Yamaguchi,³⁹ Y. Yamashita,²⁵ M. Yamauchi,⁷ Heyoung Yang,³³ J. Ying,³⁰ C. C. Zhang,⁹ L. M. Zhang,³² Z. P. Zhang,³² V. Zhilich,¹ D. Žontar,^{16,12} and D. Zürcher¹⁵

(Belle Collaboration)

¹*Budker Institute of Nuclear Physics, Novosibirsk*²*Chiba University, Chiba*³*Chonnam National University, Kwangju*⁴*University of Cincinnati, Cincinnati, Ohio 45221*⁵*Gyeongsang National University, Chinju*⁶*University of Hawaii, Honolulu, Hawaii 96822*⁷*High Energy Accelerator Research Organization (KEK), Tsukuba*⁸*Hiroshima Institute of Technology, Hiroshima*⁹*Institute of High Energy Physics, Chinese Academy of Sciences, Beijing*¹⁰*Institute of High Energy Physics, Vienna*¹¹*Institute for Theoretical and Experimental Physics, Moscow*¹²*J. Stefan Institute, Ljubljana*¹³*Korea University, Seoul*¹⁴*Kyungpook National University, Taegu*¹⁵*Swiss Federal Institute of Technology of Lausanne, EPFL, Lausanne*¹⁶*University of Ljubljana, Ljubljana*¹⁷*University of Maribor, Maribor*¹⁸*University of Melbourne, Victoria*¹⁹*Nagoya University, Nagoya*²⁰*Nara Women's University, Nara*²¹*National Central University, Chung-li*²²*National United University, Miao Li*²³*Department of Physics, National Taiwan University, Taipei*²⁴*H. Niewodniczanski Institute of Nuclear Physics, Krakow*²⁵*Nihon Dental College, Niigata*²⁶*Niigata University, Niigata*²⁷*Osaka City University, Osaka*²⁸*Osaka University, Osaka*²⁹*Panjab University, Chandigarh*³⁰*Peking University, Beijing*

³¹*Princeton University, Princeton, New Jersey 08544*³²*University of Science and Technology of China, Hefei*³³*Seoul National University, Seoul*³⁴*Sungkyunkwan University, Suwon*³⁵*University of Sydney, Sydney, New South Wales*³⁶*Tata Institute of Fundamental Research, Bombay*³⁷*Toho University, Funabashi*³⁸*Tohoku Gakuin University, Tagajo*³⁹*Tohoku University, Sendai*⁴⁰*Department of Physics, University of Tokyo, Tokyo*⁴¹*Tokyo Institute of Technology, Tokyo*⁴²*Tokyo Metropolitan University, Tokyo*⁴³*Tokyo University of Agriculture and Technology, Tokyo*⁴⁴*University of Tsukuba, Tsukuba*⁴⁵*Virginia Polytechnic Institute and State University, Blacksburg, Virginia 24061*⁴⁶*Yonsei University, Seoul*

(Received 21 March 2005; published 5 August 2005)

We report the first observation of the radiative hyperonic B decay $B^+ \rightarrow p\bar{\Lambda}\gamma$, using a 140 fb^{-1} data sample recorded on the $Y(4S)$ resonance with the Belle detector at the KEKB asymmetric energy e^+e^- collider. The measured branching fraction is $\mathcal{B}(B^+ \rightarrow p\bar{\Lambda}\gamma) = (2.16_{-0.53}^{+0.58} \pm 0.20) \times 10^{-6}$. We examine its $M_{p\bar{\Lambda}}$ distribution and observe a peak near threshold. This feature is expected by the short-distance $b \rightarrow s\gamma$ transition. A search for $B^+ \rightarrow p\bar{\Sigma}^0\gamma$ yields no significant signal, and we set a 90% confidence-level upper limit on the branching fraction of $\mathcal{B}(B^+ \rightarrow p\bar{\Sigma}^0\gamma) < 4.6 \times 10^{-6}$.

DOI: [10.1103/PhysRevLett.95.061802](https://doi.org/10.1103/PhysRevLett.95.061802)

PACS numbers: 13.20.He, 13.25.Hw, 14.40.Nd

The $b \rightarrow s\gamma$ penguin diagram is responsible for the large rates of the observed radiative $B \rightarrow K^*\gamma$ [1] decays. It is also a good probe of new physics beyond the standard model [2]. Recently, the Belle Collaboration reported a very stringent limit of $\mathcal{O}(10^{-6})$ on the branching fraction of two-body $B^+ \rightarrow p\bar{\Lambda}$ decays [3] but found an unexpectedly large rate for the three-body decay $B^0 \rightarrow p\bar{\Lambda}\pi^-$ [4], which proceeds, presumably, via the $b \rightarrow s$ penguin process. One interesting feature of the $B^0 \rightarrow p\bar{\Lambda}\pi^-$ decay is that the observed proton- $\bar{\Lambda}$ mass $M_{p\bar{\Lambda}}$ spectrum peaks near threshold. Naively, a suppression of $\mathcal{O}(\alpha_{\text{EM}})$ is expected for the $B^+ \rightarrow p\bar{\Lambda}\gamma$ decay relative to $B^+ \rightarrow p\bar{\Lambda}$ if the former process is bremsstrahlung-like. Note that the $b \rightarrow u$ transition with bremsstrahlung is also a possible process for $B^+ \rightarrow p\bar{\Lambda}\gamma$. In contrast, a short-distance $b \rightarrow s\gamma$ contribution can lead naturally to a non-bremsstrahlung-like energetic photon spectrum and an enhancement of $M_{p\bar{\Lambda}}$ at low mass; the former distribution can be compared to the recently measured $b \rightarrow s\gamma$ inclusive photon energy spectrum [5]. These features motivate our study of $B^+ \rightarrow p\bar{\Lambda}\gamma$. Theoretical predictions [6] for the branching fraction of $B^+ \rightarrow p\bar{\Lambda}\gamma$ are at the 10^{-6} level.

We use a data sample of $152 \times 10^6 B\bar{B}$ pairs, corresponding to an integrated luminosity of 140 fb^{-1} , collected by the Belle detector at the KEKB [7] asymmetric energy e^+e^- collider. The Belle detector is a large-solid-angle magnetic spectrometer that consists of a three-layer silicon vertex detector, a 50-layer central drift chamber (CDC), an array of aerogel threshold Čerenkov counters (ACC), a barrel-like arrangement of time-of-flight (TOF) scintillation counters, and an electromagnetic calorimeter (ECL)

composed of CsI(Tl) crystals located inside a superconducting solenoid coil that provides a 1.5 T magnetic field. An iron flux return located outside the coil is instrumented to detect K_L^0 mesons and to identify muons. The detector is described in detail elsewhere [8].

To identify the charged tracks, the proton (L_p), pion (L_π), and kaon (L_K) likelihoods are determined from the information obtained by the hadron identification system (CDC, ACC, and TOF). Prompt proton candidates must satisfy the requirements of $L_p/(L_p + L_K) > 0.6$ and $L_p/(L_p + L_\pi) > 0.6$, and not be associated with the decay of a Λ baryon. The proton selection efficiency is about 84% (88% for p and 80% for \bar{p}) for particles with momenta at $2 \text{ GeV}/c$. Using the $D^{*+} \rightarrow D^0\pi^+$, $D^0 \rightarrow K^-\pi^+$ control sample, the fake rate is determined to be 10% for kaons and 3% for pions.

The prompt proton candidates are also required to satisfy track quality criteria based on track impact parameters relative to the interaction point (IP). The deviations from the IP position are required to be within 0.3 cm in the transverse (x - y) plane, and within ± 3 cm in the z direction, where the z axis is opposite the direction of the positron beam. Candidate Λ baryons are reconstructed from two oppositely charged tracks, one treated as a proton and the other as a pion, and must have a mass between 1.111 and $1.121 \text{ MeV}/c^2$, as well as a displaced vertex and flight direction consistent with a Λ originating from the interaction point [3]. To reduce background, a $L_p/(L_p + L_\pi) > 0.6$ requirement is applied to the protonlike track. The mass resolution of Λ is about $1 \text{ MeV}/c^2$. Photon candidates are selected from the neutral clusters within the barrel ECL (with polar angle between 33° and 128°) having energy

greater than 500 MeV. We discard any photon candidate if the mass, in combination with any other photon above 30 (200) MeV, is within $\pm 18(\pm 32)$ MeV/ c^2 of the nominal mass of the $\pi^0(\eta)$ meson. The mass resolution of $\pi^0(\eta)$ is about 6.4(10) MeV/ c^2 .

Candidate B mesons are formed by combining a proton with a $\bar{\Lambda}$ and a photon [9], each defined using the above criteria, and requiring the beam-energy constrained mass, $M_{bc} = \sqrt{E_{\text{beam}}^2 - p_B^2}$, and the energy difference, $\Delta E = E_B - E_{\text{beam}}$, to lie in the ranges $5.2 < M_{bc} < 5.29$ GeV/ c^2 and $-0.2 < \Delta E < 0.5$ GeV. Here, p_B and E_B refer to the momentum and energy, respectively, of the reconstructed B meson, and E_{beam} refers to the beam energy, all in the $Y(4S)$ rest frame. Because of the $\Delta E > -0.2$ GeV requirement, background from B feed-down is negligible except that from $B^+ \rightarrow p\bar{\Sigma}^0\gamma$ decay where $\bar{\Sigma}$ subsequently decays to $\bar{\Lambda}\gamma$ almost 100% of the time. The $p\bar{\Sigma}^0\gamma$ events can form a nearby peak (shifted about -100 MeV in ΔE) with respect to the signal peak in the $M_{bc} - \Delta E$ region.

The dominant background for $B^+ \rightarrow p\bar{\Lambda}\gamma$ decay is from continuum $e^+e^- \rightarrow q\bar{q}$ processes, where $q = u, d, s, c$. The continuum background is evaluated with a Monte Carlo (MC) sample of 120×10^6 continuum events. In the $Y(4S)$ rest frame, continuum events are jetlike while $B\bar{B}$ events are spherical. We follow the scheme defined in Ref. [10] and combine seven shape variables to form a Fisher discriminant [11] in order to maximize the distinction between continuum processes and signal. Probability density functions (PDFs) for the Fisher discriminant and the cosine of the angle between the B flight direction and the beam direction in the $Y(4S)$ frame are combined to form the signal (background) likelihood \mathcal{L}_s (\mathcal{L}_b). We require the likelihood ratio $\mathcal{R} = \mathcal{L}_s/(\mathcal{L}_s + \mathcal{L}_b)$ to be greater than 0.75; this suppresses about 86% of the background while retaining 78% of the signal. The optimal selection requirement is determined by maximizing $N_s/\sqrt{N_s + N_b}$, where N_s and N_b denote the expected number of signal and background events; here a signal branching fraction of 4×10^{-6} is assumed.

We perform an unbinned extended maximum likelihood fit to the events with $-0.2 < \Delta E < 0.5$ GeV and $M_{bc} > 5.2$ GeV/ c^2 in order to determine the signal yield, Σ feed-down, and $q\bar{q}$ background. The extended likelihood function is defined as

$$\mathcal{L} = \frac{e^{-(N_\Lambda + N_\Sigma + N_{q\bar{q}})}}{N!} \prod_{i=1}^N [N_\Lambda P_\Lambda(M_{bc_i}, \Delta E_i) + N_\Sigma P_\Sigma(M_{bc_i}, \Delta E_i) + N_{q\bar{q}} P_{q\bar{q}}(M_{bc_i}, \Delta E_i)],$$

where N is the total number of events in the fit; P_Λ , P_Σ , and $P_{q\bar{q}}$ are the PDFs for $p\bar{\Lambda}\gamma$, $p\bar{\Sigma}^0\gamma$, and continuum background, respectively; N_Λ , N_Σ , and $N_{q\bar{q}}$ are the corresponding number of candidates.

The $p\bar{\Lambda}\gamma$ and $p\bar{\Sigma}^0\gamma$ PDFs are two-dimensional functions approximated by smooth histograms from

MC simulation. We use the parametrization first suggested by the ARGUS Collaboration [12], $f(M_{bc}) \propto M_{bc}\sqrt{1 - (M_{bc}/E_{\text{beam}})^2} \exp[-\xi(1 - (M_{bc}/E_{\text{beam}})^2)]$, to model the background M_{bc} distribution, and a quadratic polynomial for the background ΔE shape. We perform a two-dimensional unbinned fit to the ΔE vs M_{bc} distribution, with the signal and background normalizations as well as the continuum background shape parameters allowed to float.

The ΔE distribution (with $M_{bc} > 5.27$ GeV/ c^2) and the M_{bc} distribution (with $-0.135 < \Delta E < 0.074$ GeV) for the region $M_{p\bar{\Lambda}} < 2.4$ GeV/ c^2 are shown in Fig. 1 along with the projections of the fit. The two-dimensional unbinned fit gives a $B^+ \rightarrow p\bar{\Lambda}\gamma$ signal yield of $34.1_{-6.6}^{+7.1}$ with a statistical significance of 8.6 standard deviations and a $B^+ \rightarrow p\bar{\Sigma}^0\gamma$ yield of 0.0 ± 4.7 . The significance is defined as $\sqrt{-2 \ln(L_0/L_{\text{max}})}$, where L_0 and L_{max} are the likelihood values returned by the fit with signal yield fixed at zero and its best fit value, respectively.

We measure the differential branching fraction of $p\bar{\Lambda}\gamma$ by fitting the yield in bins of $M_{p\bar{\Lambda}}$, as shown in Fig. 2, and correcting for the corresponding detection efficiency as determined from a large MC sample of events distributed uniformly in phase space. The results of the fits along with the efficiencies and the partial branching fractions are given in Table I. In these fits, the signal yields are constrained to be non-negative. The yield is consistent with null signal for higher $M_{p\bar{\Lambda}}$ bins if the non-negative constraint is removed. The observed mass distribution in Fig. 2 peaks at low $p\bar{\Lambda}$ mass, a feature seen also in $B^0 \rightarrow p\bar{\Lambda}\pi^-$ and $B^+ \rightarrow p\bar{p}K^+$ decays [4,13].

We also study the angular distribution of the proton in the baryon pair system. The angle θ_χ is measured between the proton direction and the γ direction in the baryon pair rest frame. Figure 3 shows the efficiency corrected B yield in bins of $\cos\theta_\chi$ for $M_{p\bar{\Lambda}} < 4.0$ GeV/ c^2 . Note that the total B yield differs from that in Table I due to the fit procedure

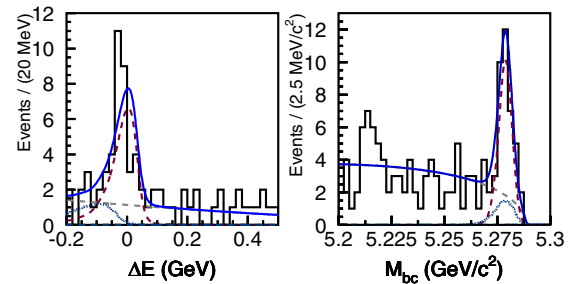


FIG. 1 (color online). The distributions of ΔE (for $M_{bc} > 5.27$ GeV/ c^2) and M_{bc} (for $-0.135 < \Delta E < 0.074$ GeV) for $B^0 \rightarrow p\bar{\Lambda}\gamma$ candidates having $M_{p\bar{\Lambda}} < 2.4$ GeV/ c^2 . The solid, light dashed, and dark dashed lines represent the combined fit result, fitted background, and fitted signal, respectively. The dotted lines represent projections of 10 assumed $p\bar{\Sigma}^0\gamma$ events for comparison.

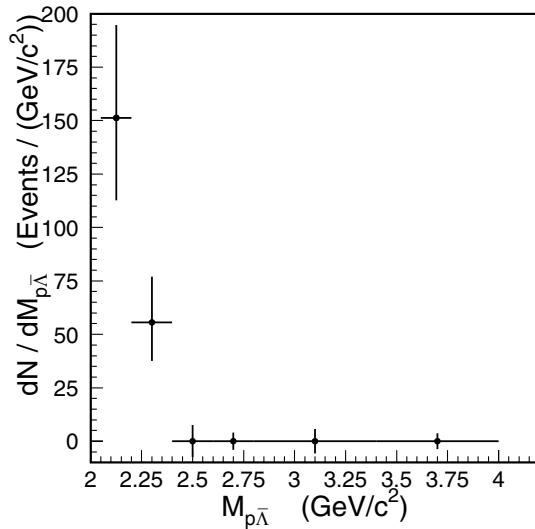


FIG. 2. The differential yield for $B^0 \rightarrow p\bar{\Lambda}\gamma$ as a function of $M_{p\bar{\Lambda}}$.

with positive yield requirement and float background PDF. This distribution supports the $b \rightarrow s\gamma$ fragmentation picture where the Λ tends to emerge opposite the direction of the photon. We define the angular asymmetry as $A = \frac{N_{\cos\theta_X+} - N_{\cos\theta_X-}}{N_{\cos\theta_X+} + N_{\cos\theta_X-}}$, where $N_{\cos\theta_X+}$ and $N_{\cos\theta_X-}$ stand for the efficiency corrected B yield with $\cos\theta_X > 0$ and $\cos\theta_X < 0$, respectively. The measured value for A is $0.36_{-0.20}^{+0.23}$.

The systematic uncertainty in particle selection is studied using high statistics control samples. Proton identification is studied with a $\Lambda \rightarrow p\pi^-$ sample. The tracking efficiency is studied with a D^* sample, using both full and partial reconstruction. Based on these studies, we sum the correlated errors linearly and assign a 4.1% error for proton identification and 4.9% for the tracking efficiency.

For Λ reconstruction, we have an additional uncertainty of 2.5% on the efficiency for tracks away from the interaction point. This is determined from the difference of Λ proper time distributions for data and MC simulation. There is also a 1.2% error associated with the Λ mass selection and a 0.5% error for the Λ vertex selection.

TABLE I. The event yield, efficiency, and branching fraction (\mathcal{B}) for each $M_{p\bar{\Lambda}}$ bin.

$M_{p\bar{\Lambda}}$ (GeV/ c^2)	Signal yield	Efficiency (%)	$\mathcal{B}(10^{-6})$
<2.2	$22.7_{-5.8}^{+6.5}$	10.6	$1.41_{-0.36}^{+0.40}$
2.2–2.4	$11.1_{-3.6}^{+4.3}$	9.8	$0.74_{-0.24}^{+0.29}$
2.4–2.6	$0.0_{-1.5}^{+1.5}$	9.3	$0.00_{-0.11}^{+0.11}$
2.6–2.8	$0.0_{-0.8}^{+0.8}$	9.9	$0.00_{-0.06}^{+0.06}$
2.8–3.4	$0.0_{-3.4}^{+3.4}$	9.6	$0.00_{-0.23}^{+0.23}$
3.4–4.0	$0.0_{-2.2}^{+2.2}$	9.6	$0.00_{-0.15}^{+0.15}$
Total	$33.8_{-8.1}^{+9.0}$...	$2.16_{-0.53}^{+0.58}$

Summing the errors for Λ reconstruction, we obtain a systematic error of 2.8%.

The 2.2% uncertainty for the photon detection is determined from radiative Bhabha events. For the π^0 and η vetoes, we compare the fit results with and without the vetoes; the difference in the branching fraction is 0.5%, which is taken as the associated systematic error.

Continuum suppression is studied by varying the selection criteria on \mathcal{R} in the interval 0–0.9 to see if there is any systematic trend in the signal fit yield. We quote a 2.5% error for this.

The systematic uncertainty from fitting is 2.2%, which is determined by assuming uncorrelated M_{bc} and ΔE PDFs, and by varying the parameters of the signal and background PDFs. The MC statistical uncertainty and modeling with six $M_{p\bar{\Lambda}}$ bins contributes a 4.4% error (obtained by changing the $M_{p\bar{\Lambda}}$ bin size). The error on the number of total $B\bar{B}$ pairs is 0.5%. The error from the subdecay branching fraction of $\Lambda \rightarrow p\pi^-$ is 0.8% [14].

We combine the above uncorrelated errors in quadrature. The total systematic error is 9.2%.

We see no evidence for the decay $B^+ \rightarrow p\bar{\Sigma}^0\gamma$. We use the fit results to estimate the expected background, and compare this with the observed number of events in the $p\bar{\Sigma}^0\gamma$ signal region ($-0.20 \text{ GeV} < \Delta E < 0.04 \text{ GeV}$ and $M_{bc} > 5.27 \text{ GeV}/c^2$) in order to set an upper limit on the yield [15]. The estimated background for $M_{p\bar{\Lambda}} < 4.0 \text{ GeV}/c^2$ is 84.0 ± 9.2 , the number of observed events is 96, and the systematic uncertainty is 9.2%; from these, the upper limit yield is 35.5 at 90% confidence level. Assuming the $B^0 \rightarrow p\bar{\Sigma}^0\gamma$ three-body decay is uniform in phase space, the overall efficiency including the loss from the $M_{p\bar{\Lambda}} < 4.0 \text{ GeV}/c^2$ requirement is 5.1%; the 90% confidence-level upper limit for the branching fraction is $\mathcal{B}(B^0 \rightarrow p\bar{\Sigma}^0\gamma) < 4.6 \times 10^{-6}$. Using a $b \rightarrow s\gamma$ model and selecting events with $M_{p\bar{\Lambda}} < 2.4 \text{ GeV}/c^2$, we

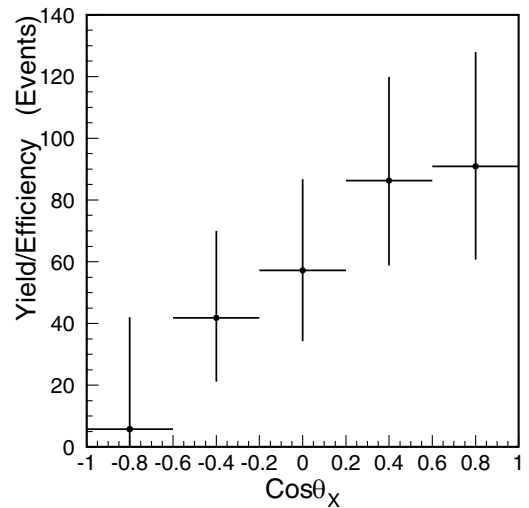


FIG. 3. Efficiency corrected yield versus $\cos\theta_X$ in the baryon pair system.

can obtain a more stringent upper limit yield, 14.9, with an estimated efficiency of 6.7%. The 90% confidence-level upper limit becomes $\mathcal{B}(B^0 \rightarrow p\bar{\Sigma}^0\gamma) < 1.5 \times 10^{-6}$.

In summary, we have performed a search for the radiative baryonic decays $B^+ \rightarrow p\bar{\Lambda}\gamma$ and $p\bar{\Sigma}^0\gamma$ with $152 \times 10^6 B\bar{B}$ events. A clear signal is seen in the $p\bar{\Lambda}\gamma$ mode, and we measure a branching fraction of $\mathcal{B}(B^+ \rightarrow p\bar{\Lambda}\gamma) = (2.16_{-0.53}^{+0.58}(\text{stat}) \pm 0.20(\text{syst})) \times 10^{-6}$, which is consistent with the upper limit set by CLEO [16]. The short-distance $b \rightarrow s\gamma$ transition can describe the observed $M_{p\bar{\Lambda}}$ spectrum and proton angular distribution naturally. The yield of the $B^0 \rightarrow p\bar{\Sigma}^0\gamma$ mode is not statistically significant, and we set the 90% confidence-level upper limit of $\mathcal{B}(B^0 \rightarrow p\bar{\Sigma}^0\gamma) < 4.6 \times 10^{-6}$ for phase space model ($< 1.5 \times 10^{-6}$ for threshold peaking model). The measured branching fractions of these two radiative B decays are consistent with theoretical expectations [6].

We thank the KEKB group for the excellent operation of the accelerator, the KEK cryogenics group for the efficient operation of the solenoid, and the KEK computer group and the National Institute of Informatics for valuable computing and Super-SINET network support. We acknowledge support from the Ministry of Education, Culture, Sports, Science and Technology of Japan and the Japan Society for the Promotion of Science; the Australian Research Council and the Australian Department of Education, Science and Training; the National Science Foundation of China under Contract No. 10175071; the Department of Science and Technology of India; the BK21 program of the Ministry of Education of Korea and the CHEP SRC program of the Korea Science and Engineering Foundation; the Polish State Committee for Scientific Research under Contract No. 2P03B 01324; the Ministry of Science and Technology of the Russian Federation; the Ministry of Higher Education, Science and Technology of the Republic of Slovenia; the Swiss National Science Foundation; the National Science Council and the

Ministry of Education of Taiwan; and the U.S. Department of Energy.

*On leave from Nova Gorica Polytechnic, Nova Gorica.

- [1] R. Ammar *et al.* (CLEO Collaboration), Phys. Rev. Lett. **71**, 674 (1993); B. Aubert *et al.* (BABAR Collaboration), Phys. Rev. Lett. **88**, 101805 (2002); M. Nakao *et al.* (Belle Collaboration), Phys. Rev. D **69**, 112001 (2004).
- [2] T. Hurth, E. Lunghi, and W. Porod, Nucl. Phys. **B704**, 56 (2005), and references therein.
- [3] K. Abe *et al.* (Belle Collaboration), Phys. Rev. D **65**, 091103 (2002).
- [4] M.-Z. Wang *et al.* (Belle Collaboration), Phys. Rev. Lett. **90**, 201802 (2003).
- [5] P. Koppenburg *et al.* (Belle Collaboration), Phys. Rev. Lett. **93**, 061803 (2004).
- [6] Wei-Shu Hou and A. Soni, Phys. Rev. Lett. **86**, 4247 (2001); H. Y. Cheng and K. C. Yang, Phys. Lett. B **533**, 271 (2002); C. Q. Geng and Y. K. Hsiao, Phys. Lett. B **610**, 67 (2005).
- [7] S. Kurokawa and E. Kikutani, Nucl. Instrum. Methods Phys. Res., Sect. A **499**, 1 (2003).
- [8] A. Abashian *et al.* (Belle Collaboration), Nucl. Instrum. Methods Phys. Res., Sect. A **479**, 117 (2002).
- [9] Throughout this Letter, inclusion of charge conjugate modes is always implied unless otherwise stated.
- [10] K. Abe *et al.* (Belle Collaboration), Phys. Lett. B **517**, 309 (2001).
- [11] R. A. Fisher, Ann. Eugenics **7**, 179 (1936).
- [12] H. Albrecht *et al.*, Phys. Lett. B **241**, 278 (1990); **254**, 288 (1991).
- [13] M.-Z. Wang *et al.* (Belle Collaboration), Phys. Rev. Lett. **92**, 131801 (2004).
- [14] S. Eidelman *et al.* (Particle Data Group), Phys. Lett. B **592**, 1 (2004).
- [15] J. Conrad *et al.*, Phys. Rev. D **67**, 012002 (2003).
- [16] K. W. Edwards *et al.* (CLEO Collaboration), Phys. Rev. D **68**, 011102 (2003).